Weierstraß-Institut
für Angewandte Analysis und Stochastik

im Forschungsverbund Berlin e.V.

Preprint ISSN 0946 – 8633

Simulations of 3D/4D precipitation processes in a turbulent flow field

Volker John [1], Michael Roland [2]

submitted: 23rd November 2009

[1] Weierstrass Institute for Applied Analysis and Stochastics Mohrenstr. 39, 10117 Berlin, Germany
and Free University of Berlin, Department of Mathematics and Computer Science
Arnimallee 14, 14195 Berlin, Germany
e-mail: john@wias-berlin.de

[2] Saarland University, FR 6.1 - Mathematics, Postfach 15 11 50, 66041 Saarbrücken, Germany
email: roland@math.uni-sb.de

No. 1463
Berlin 2009

2010 *Mathematics Subject Classification.* 76F65, 65M06, 65M60.

Key words and phrases. population balance system, precipitation process, incompressible Navier–Stokes equations, transport equations, FEM–FCT scheme, upwind finite difference method.

Edited by
Weierstraß-Institut für Angewandte Analysis und Stochastik (WIAS)
Mohrenstraße 39
10117 Berlin
Germany

Fax: + 49 30 2044975
E-Mail: preprint@wias-berlin.de
World Wide Web: http://www.wias-berlin.de/

Abstract

Precipitation processes are modeled by population balance systems. A very expensive part of the simulation of population balance systems is the solution of the equation for the particle size distribution (PSD) since this equation is defined in a higher dimensional domain than the other equations in the system. This paper studies different approaches for the solution of this equation: two finite difference upwind schemes and a linear finite element flux–corrected transport method. It is shown that the different schemes lead to qualitatively different solutions for an output of interest.

1 Introduction

Precipitation processes describe nucleation, growth, breakage, agglomeration and transport of particles in a fluid. They are very important in the chemical industry. Already a decade ago, over 50% of the products in chemical engineering were produced in particulate form [18]. Since that time, the importance of particulate products has been even increased. Nowadays, the main focus is on the production of particles with prescribed characteristics, such as size, shape or chemical properties. The numerical simulation of precipitation processes will make an essential contribution to the optimization of the production process.

Isothermal precipitation processes are modeled by a coupled system of the Navier–Stokes equations to describe the flow field, of convection–diffusion–reaction

equations to describe the transport and the reaction of the chemical species and of a transport equation for the particle size distribution (PSD).

The flow field in applications is often turbulent. The numerical simulation of turbulent flows is by itself an active field of research [1, 6, 17]. In the numerical simulations presented in this paper, a finite element variational multiscale (VMS) method will be used [7]. VMS methods are a rather new approach for turbulence modeling, which were derived from general principles for simulating multiscale phenomena [3, 4].

A chemical reaction happens in the flow field which is modeled by a nonlinear system of convection–diffusion–reaction equations. These equations are convection– and reaction–dominated. Also the numerical simulation of this type of equations is by itself an active field of research [16].

The main feature of precipitation processes is the nucleation of particles if the concentration of a species exceeds a saturation concentration. In applications, not the behavior of the individual particles is of interest, but the PSD. The PSD depends not only on time and space, but also on properties of the particles, so–called internal coordinates. Thus, the transport equation for the PSD is defined in a higher dimensional domain than the other equations of the coupled system.

The simulations presented in this paper will consider the flow of a dilute solution. Hence, the effect of the particles on the flow field are negligible. Nucleation and growth of particles, which are the most important chemical mechanisms in a precipitation process, are included into the used model. Breakage and agglomeration of particles will not be part of the model, because they are of much less importance and the growth process of the particles in this model is realized by layering [15]. The PSD has one internal coordinate, namely the diameter of the particles.

The simulation of complex coupled systems is generally rather time–consuming. In simulations of precipitation processes, a very expensive part will be the solution of the higher–dimensional PSD equation. This paper will study different schemes for discretizing this equation: on the one hand rather inexpensive but also inaccurate schemes and on the other hand a more expensive but also more accurate scheme. It will be demonstrated that the use of the different schemes leads to qualitatively different results for an output of interest.

2 The model of the precipitation process

For shortness of presentation, we will give here only the non–dimensionalized model, see [10, 11] for its derivation.

Let Ω be the flow domain and T a final time. We will consider a dilute fluid, i.e. the number of particles and their size are sufficiently small such that their influence on the flow field can be neglected. Then, the Navier–Stokes equations are given by

$$\frac{\partial \mathbf{u}}{\partial t} - \frac{1}{Re}\Delta \mathbf{u} + (\mathbf{u}\cdot\nabla)\mathbf{u} + \nabla p = \mathbf{0} \text{ in } (0,T]\times\Omega, \tag{1}$$

$$\nabla\cdot\mathbf{u} = 0 \text{ in } [0,T]\times\Omega, \tag{2}$$

where $\mathbf{u}$ is the velocity, p is the pressure and $Re = u_\infty l_\infty / \nu$ is the Reynolds number with l_∞ being a characteristic length scale and u_∞ a characteristic velocity scale of the problem. Let c_A and c_B be the concentrations of the reactants A and B, then their reaction is described by the following equations

$$\frac{\partial c_i}{\partial t} - \frac{D_i}{u_\infty l_\infty} \Delta c_i + \mathbf{u} \cdot \nabla c_i + k_R \frac{l_\infty c_\infty}{u_\infty} c_A c_B = 0 \text{ in } (0,T] \times \Omega, \tag{3}$$

$i \in \{A,B\}$, where D_i is a diffusion coefficient, k_R is the reaction rate constant and c_∞ is a characteristic concentration scale for the reactants. The equation for the concentration of the dissolved product C is given by

$$\begin{aligned} \frac{\partial c_C}{\partial t} - \frac{D_C}{u_\infty l_\infty} \Delta c_C + \mathbf{u} \cdot \nabla c_C - \Lambda_{\text{chem}} c_A c_B + \Lambda_{\text{nuc}} \max\left\{0, (c_C - 1)^5\right\} \\ + \left(c_C - \frac{c_{C,\infty}^{\text{sat}}}{c_{C,\infty}} \right) \int_{d_{\text{p,min}}}^{1} d_{\text{p}}^2 f \, \mathrm{d}(d_{\text{p}}) = 0 \text{ in } (0,T] \times \Omega. \end{aligned} \tag{4}$$

Here, D_C is a diffusion constant, d_{p} describes the size of the particles, f denotes the PSD, $c_{C,\infty}^{\text{sat}}$ is the saturation concentration of the dissolved product C and $c_{C,\infty} = c_{C,\infty}^{\text{sat}} \exp(C_2 / \widetilde{d}_{\text{p,0}})$ is a characteristic concentration scale for C with C_2 being a model constant and $\widetilde{d}_{\text{p,0}}$ ($\widetilde{d}_{\text{p,max}}$) being the smallest (largest) possible particle diameter. The parameters in (4) are

$$\Lambda_{\text{chem}} = k_R \frac{c_\infty^2 l_\infty}{c_{C,\infty} u_\infty}, \quad d_{\text{p,min}} = \frac{\widetilde{d}_{\text{p,0}}}{d_{\text{p},\infty}}, \quad \Lambda_{\text{nuc}} = C_{\text{nuc}} d_{\text{p,min}}^3 d_{\text{p},\infty}^3 k_{\text{nuc}} \frac{l_\infty c_{C,\infty}^4}{u_\infty},$$

with $d_{\text{p},\infty}$ being an upper bound for the largest possible particle diameter and C_{nuc} and k_{nuc} are constants in the model for the nucleation process. To obtain the last term on the left hand side of (4) in the presented form, the characteristic scale of the PSD $f_\infty = u_\infty / (C_G k_G d_{\text{p},\infty}^3 l_\infty)$ was used, where C_G is a constant to model the growth of the particles and k_G is a growth rate constant. The last equation describes the PSD

$$\frac{\partial f}{\partial t} + \mathbf{u} \cdot \nabla f + G(c_C) \frac{l_\infty}{u_\infty d_{\text{p},\infty}} \frac{\partial f}{\partial d_{\text{p}}} = 0 \text{ in } (0,T] \times \Omega \times \left(d_{\text{p,min}}, \frac{\widetilde{d}_{\text{p,max}}}{d_{\text{p},\infty}} \right) \tag{5}$$

with the growth rate $G(c_C) = k_G c_{C,\infty} (c_C - c_{C,\infty}^{\text{sat}} / c_{C,\infty})$.

In summary, the coupled system of equations (1), (2), (3) for c_A, (3) for c_B, (4) and (5) has to be solved. All equations have to be equipped with initial and boundary conditions.

3 The applied numerical methods

The Crank–Nicolson scheme with an equidistant time step is applied as temporal discretization for the equations (1) – (4).

In the considered system, the velocity $\mathbf{u}$ is needed in all other equations but the other quantities do not influence the Navier–Stokes equations. For this reason, a straightforward approach consists in solving at each discrete time first (1), (2). The velocity is approximated with the Q_2 finite element and the pressure with the P_1^{disc} finite element, i.e. with discontinuous piecewise linears. The simulations will study a turbulent flow, hence a turbulence model has to be applied. We will use the projection–based finite element variational multiscale method from [7] with a piecewise constant large scale space, see [8] for an adaptive choice of the large scale space.

With the obtained velocity field, the system for the concentrations c_A and c_B can be solved. This is done by a fixed point iteration. The linearized equations are discretized with the Q_1 finite element. They are strongly convection–dominated such that a stabilization has to be applied. Comparative studies of stabilized finite element schemes [12, 13] have shown that for the Q_1 finite element FEM–FCT (flux–corrected transport) schemes outperform more standard approaches like SUPG. In the simulations presented in Section 4, a linear FEM–FCT scheme from [14] is used.

After having computed c_A and c_B, a coupled system for c_C and f remains. This system is decoupled and linearized in our approach by treating (4) in a semi–implicit way, namely by using c_C and the PSD f from the previous discrete time in the last two terms on the left hand side of (4). Thus (4) becomes a linear equation in each discrete time, which is solved also with a linear Q_1–FEM–FCT scheme.

The emphasis of the numerical studies is on the schemes for the PSD equation (5). This equation is given in a 4D domain and its solution might be rather expensive. For this reason, one can think about using comparatively cheap but also rather inaccurate schemes for (5). The first scheme of this kind which we apply is the forward Euler simple upwind finite difference scheme. The second scheme, the backward Euler simple upwind finite difference scheme, is only somewhat more expensive. The results and the costs of these schemes will be compared with the much more expensive linear Q_1–FEM–FCT scheme.

4 Numerical studies

The calcium carbonate precipitation $Na_2CO_3 + CaCl_2 \longrightarrow CaCO_3 \downarrow + 2NaCl$ is considered in the numerical studies. The parameters of this process are given by

- $\nu = 10^{-6}$ m^2/s
- $\rho = 1$ kg/m^3
- $k_G = 10^{-7}$ m^4/kmol s
- $k_{\text{nuc}} = 10^{24}$ (1/m^3 s)/(kmol/m^3)^5
- $k_R = 10^{-2}$ m^3/kmol s
- $c_{C,\infty}^{\text{sat}} = 1.37\ 10^{-4}$ kmol/m^3
- $C_2 = 7.2\ 10^{-9}$ m
- $C_G = 45.98$ kmol/m^3
- $C_{\text{nuc}} = 15.33$ kmol/m^3
- $D_A = D_B = D_C = 1.5\ 10^{-9}$ m^2/s
- $\widetilde{d}_{\text{p},0} = 10^{-9}$ m
- $\widetilde{d}_{\text{p,max}} = 10^{-4}$ m.

The following reference quantities have been used in the dimensionless equations:

- $l_\infty = 1$ m
- $u_\infty = 10^{-2}$ m/s
- $t_\infty = 10^2$ s
- $c_\infty = 1$ kmol/m^3
- $c_{C,\infty} = 0.183502$ kmol/m^3
- $d_{\text{p},\infty} = 10^{-4}$ m
- $f_\infty = 2.17486\ 10^{15}$ 1/m^4.

Concerning the flow, a situation similar to a driven cavity problem is considered. The flow domain is $(0,1)^3$. There are opposite inlets at $\{0\} \times (0.4375, 0.5625) \times (0.4375, 0.5625)$ and $\{1\} \times (0.4375, 0.5625) \times (0.4375, 0.5625)$ and an outlet at $(0.4375, 0.5625) \times (0.4375, 0.5625) \times \{0\}$. A situation like this is sometimes called T–mixer. The inflows are given by a profile which was precomputed by solving the Poisson equation with right hand side equal to the constant 1 on the inlets and with homogeneous Dirichlet boundary conditions. On the top of the cavity, the velocity $(1,0,0)^T$ is prescribed, outflow boundary conditions are given at the outlet and no slip boundary conditions on the remaining boundaries. Initially, the fluid was considered to be at rest and an impulsive start was performed. The Reynolds number of the flow is $Re = 10000$. Even the driven cavity problem without inlets and outlet is a turbulent flow at this Reynolds number [2, 5].

All concentrations inside the domain were zero at the initial time. On the boundary, the concentrations of the reactants A at the left inlet and B at the right inlet were set to 1 for all times. Homogeneous Neumann boundary conditions were used on all other parts of the boundary. For the substance C, homogeneous Neumann boundary conditions were applied on the whole boundary. The boundary condition for the PSD with respect to the internal coordinate was

$$\begin{aligned} f(t,x_1,x_2,x_3,d_{\text{p,min}}) &= \frac{B_{\text{nuc}}(c_C)}{f_\infty G(c_C)} && \text{if } G(c_C(t,x_1,x_2,x_3)) > 0, \\ f(t,x_1,x_2,x_3,d_{\text{p,min}}) &= 0 && \text{if } G(c_C(t,x_1,x_2,x_3)) = 0, \\ f(t,x_1,x_2,x_3,d_{\text{p,max}}) &= 0 && \text{if } G(c_C(t,x_1,x_2,x_3)) < 0, \end{aligned}$$

with the nucleation rate $B_{\text{nuc}}(c_C) = k_{\text{nuc}} c_{C,\infty}^5 \max\{0, (c_C - 1)^5\}$. With respect to the spatial coordinates, the PSD was set to be zero at the closure of the fluid flow inlets (no particles enter through the inlets).

The length of the time step was set to be $\Delta t = 0.001$. In space, a $16 \times 16 \times 16$ uniform mesh consisting of cubes was used which leads to 107 811 velocity d.o.f., 16 384 pressure d.o.f. and 4913 d.o.f. for the concentrations. The internal coordinate was discretized with 64 nodes (319 345 d.o.f.) , were the mesh finer small diameters. Figure 1 shows the flow field and isosurfaces of the concentrations at around the starting time of the precipitation process. The flow field and the concentrations c_A, c_B, are always the same for all discretizations of the PSD equation. Until the start

of the precipitation, i.e. until the back coupling of f onto c_C starts, the concentration c_C is also identical for all discretizations of (5).

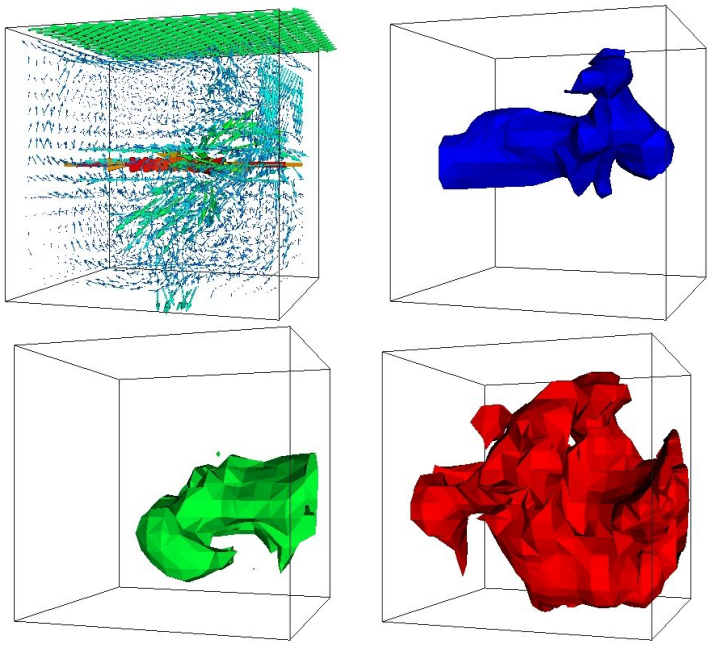

Fig. 1 Velocity field, isosurfaces for $c_A = 0.25$, $c_B = 0.25$, $c_C = 0.7$ at $t = 32$, left to right, top to bottom.

An output of interest is the median of the volume fraction at the center of the outlet. The volume fraction and the cumulative volume fraction are given by

$$q_3(\widetilde{t},\widetilde{d}_\mathrm{p}) := \frac{\widetilde{d}_\mathrm{p}^3 \widetilde{f}(\widetilde{t},0.5,0.5,0,\widetilde{d}_\mathrm{p})}{\int_{\widetilde{d}_{\mathrm{p},0}}^{\widetilde{d}_{\mathrm{p,max}}} \widetilde{d}_\mathrm{p}^3 \widetilde{f}(\widetilde{t},0.5,0.5,0,\widetilde{d}_\mathrm{p}) \,\mathrm{d}(\widetilde{d}_\mathrm{p})}, \; Q_3(\widetilde{t},\widetilde{d}_\mathrm{p}) := \int_{\widetilde{d}_{\mathrm{p},0}}^{\widetilde{d}} q_3(\widetilde{t},\widetilde{d}_\mathrm{p}) \,\mathrm{d}(\widetilde{d}_\mathrm{p}).$$

Then, the median of the volume fraction is defined to be the particle size for which $Q_3(\widetilde{t},\widetilde{d}_\mathrm{p})$ takes the value 0.5: $\widetilde{d}_{\mathrm{p},50}(\widetilde{t}) := \{\widetilde{d}_\mathrm{p} \; : \; Q_3(\widetilde{t},\widetilde{d}_\mathrm{p}) = 0.5\}$.

The temporal developments of $\widetilde{d}_{\mathrm{p},50}(\widetilde{t})$ for the different schemes of discretizing the PSD equation (5) are presented in Figure 2. It can be seen that the first particles reach the center of the outlet at around 3200 s. The main observation is that the different numerical schemes lead to qualitatively different results. The forward Euler and the backward Euler upwind finite difference schemes predict values of $\widetilde{d}_{\mathrm{p},50}(\widetilde{t})$ at 7500 s in the range of 23 μm. The median predicted with the linear FEM–FCT scheme is less than half this value.

In a numerical study at a coupled 2D/3D problem with prescribed solution in [11] it has been shown that the FEM–FCT scheme leads to considerably more accurate results than both finite difference upwind schemes. Based on this experience, it can be expected that the results with the FEM–FCT scheme for solving the PSD equation are more reliable.

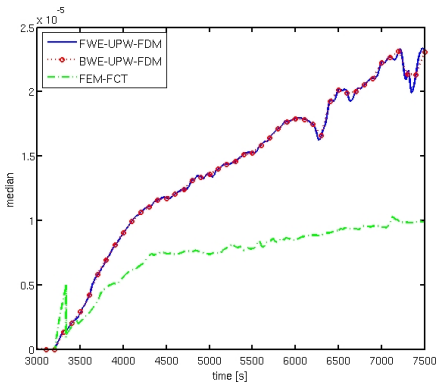

Fig. 2 Median of the volume fraction at the center of the outlet.

The numerical studies were performed with the code *MooNMD* [9]. This is a flexible research code which is not tailored for solving population balance systems. The average computing times for a time step are given in Table 1. It can be observed that the use of the forward difference upwind schemes is considerably less time–consuming.

Some numerical studies for 2D/3D population balance systems with a structured laminar flow field were performed in [11]. It was shown that in this case the results obtained with the different discretization schemes for the PSD equation were rather similar. This suggests that the reason for the qualitatively different results is the presence of the turbulent flow field, compare also some other studies in [11].

5 Summary

The paper studied different discretization schemes for the higher dimensional transport equation in a 3D/4D population balance system with a turbulent flow field. It was demonstrated that the usage of inexpensive but inaccurate schemes on the one hand and a more expensive but also more accurate scheme on the other hand leads to qualitatively different results for an output of interest. This is similar to the observations in simulations of 2D/3D population balance systems with a highly time–dependent flow field in [11].

Table 1 Average computing times per time step, computer with Intel Xeon CPU, 2.4 GHz.

scheme for solving (5)	computing time in s
forward Euler upwind FDM	19.1
backward Euler upwind FDM	23.2
Crank–Nicolson FEM–FCT	60.3

The presented simulations demonstrate that outputs of interest in the simulation of complex processes might highly depend on the applied numerical schemes. They emphasize the need of using accurate schemes and the necessity of implementing them such that they work efficiently. Our future work will focus on these topics.

References

1. L.C. Berselli, T. Iliescu, and W.J. Layton. *Mathematics of Large Eddy Simulation of Turbulent Flows*. Springer–Verlag, 2006.
2. V. Gravemeier, W.A. Wall, and E. Ramm. Large eddy simulation of turbulent incompressible flows by a three–level finite element method. *Int. J. Numer. Meth. Fluids*, 48:1067 – 1099, 2005.
3. J.-L. Guermond. Stabilization of Galerkin approximations of transport equations by subgrid modeling. *M2AN*, 33:1293 – 1316, 1999.
4. T.J.R. Hughes. Multiscale phenomena: Green's functions, the Dirichlet-to-Neumann formulation, subgrid-scale models, bubbles and the origin of stabilized methods. *Comp. Meth. Appl. Mech. Engrg.*, 127:387 – 401, 1995.
5. T. Iliescu, V. John, W.J. Layton, G. Matthies, and L. Tobiska. A numerical study of a class of LES models. *Int. J. Comput. Fluid Dyn.*, 17:75 – 85, 2003.
6. V. John. *Large Eddy Simulation of Turbulent Incompressible Flows. Analytical and Numerical Results for a Class of LES Models*, volume 34 of *Lecture Notes in Computational Science and Engineering*. Springer–Verlag Berlin, Heidelberg, New York, 2004.
7. V. John and S. Kaya. A finite element variational multiscale method for the Navier-Stokes equations. *SIAM J. Sci. Comp.*, 26:1485 – 1503, 2005.
8. V. John and A. Kindl. A variational multiscale method for turbulent flow simulation with adaptive coarse space. *J. Comput. Phys.*, 2009. in press.
9. V. John and G. Matthies. MooNMD - a program package based on mapped finite element methods. *Comput. Visual. Sci.*, 6:163 – 170, 2004.
10. V. John, T. Mitkova, M. Roland, K. Sundmacher, L. Tobiska, and A. Voigt. Simulations of population balance systems with one internal coordinate using finite element methods. *Chem. Engrg. Sci.*, 64:733 – 741, 2009.
11. V. John and M. Roland. On the impact of the scheme for solving the higher–dimensional equation in coupled population balance systems. Preprint 224, Universität des Saarlandes, FR 6.1 – Mathematik, 2008.
12. V. John and E. Schmeyer. Stabilized finite element methods for time–dependent convection–diffusion–reaction equations. *Comput. Methods Appl. Mech. Engrg.*, 198:475 – 494, 2008.
13. V. John and E. Schmeyer. On finite element methods for 3d time–dependent convection–diffusion–reaction equations with small diffusion. In *BAIL 2008 – Boundary and Interior Layers*, volume 69 of *Lecture Notes in Computational Science and Engineering*, pages 173 – 182. Springer, 2009.
14. D. Kuzmin. Explicit and implicit FEM–FCT algorithms with flux linearization. *J. Comput. Phys.*, 228:2517 – 2534, 2009.
15. K.C. Link and E.-U. Schlünder. Wirbelschicht–Sprühgranulation – Untersuchung des Coatingvorganges am frei schwebenden Einzelpartikel. *Chemie Ingenieur Technik*, 68:1139, 1996.
16. H.-G. Roos, M. Stynes, and L. Tobiska. *Robust Numerical Methods for Singularly Perturbed Differential Equations*, volume 24 of *Springer Series in Computational Mathematics*. Springer, 2nd edition, 2008.
17. P. Sagaut. *Large Eddy Simulation for Incompressible Flows*. Springer–Verlag, Berlin, Heidelberg New York, 3rd edition, 2006.
18. K. Wintermantel. Process and product engineering – achievements, present and future challenges. *Chem. Engrg. Sci.*, 54:1601 – 1620, 1999.